Study on the influencing factors of space charge dynamic behavior in XLPE insulation under alternating current electric field

Zhe Xu, Dongxin He, Hongshun Liu, Qingquan Li, Qingjing Zang, Séverine Le Roy, Gilbert Teyssèdre

▶ **To cite this version:**

Zhe Xu, Dongxin He, Hongshun Liu, Qingquan Li, Qingjing Zang, et al.. Study on the influencing factors of space charge dynamic behavior in XLPE insulation under alternating current electric field. Journal of Physics D: Applied Physics, 2022, 55 (24), pp.245302. 10.1088/1361-6463/ac5d01 . hal-03787383

HAL Id: hal-03787383
https://hal.science/hal-03787383

Submitted on 24 Sep 2022

HAL is a multi-disciplinary open access archive for the deposit and dissemination of scientific research documents, whether they are published or not. The documents may come from teaching and research institutions in France or abroad, or from public or private research centers.

L'archive ouverte pluridisciplinaire **HAL**, est destinée au dépôt et à la diffusion de documents scientifiques de niveau recherche, publiés ou non, émanant des établissements d'enseignement et de recherche français ou étrangers, des laboratoires publics ou privés.

Study on the influencing factors of space charge dynamic behavior in XLPE insulation under alternating current electric field

Zhe Xu[1], Dong He[1], Hongshun Liu[1], Qingquan Li[1], Qingjing Zang[1], Séverine Le Roy[2], and Gilbert Teyssèdre[2]

[1] *Shandong Provincial Key Laboratory of UHV Transmission Technology and Equipment, School of Electrical Engineering, Shandong University, Jinan 250061, China*

[2] *University of Toulouse; UPS, INPT, CNRS; LAPLACE (Laboratoire Plasma et Conversion d'Energie); 118 Route de Narbonne, F-31062 Toulouse Cedex 9, France*

Cite as: Z. Xu, D.X. He, H.S. Liu, Q.Q. Li, Q.J. Zang, S. Le Roy, G. Teyssèdre, "Study on the influencing factors of space charge dynamic behavior in XLPE insulation under alternating current electric field", J. Phys. D 55, 245302-1/13, 2022

Abstract *- The dynamic behavior of space charges is one of the potential factors that cause electrical aging. In this paper, a bipolar space charge transport model was established under an AC electric field in cross-linked polyethylene. The effects of physical parameters on the dynamic behavior of space charges in an AC electric field were explored by changing the injection barrier heights, mobilities, trapping coefficients, and detrapping barrier heights of positive and negative charges. The effects of voltage conditions on space charge behavior were explored by changing the amplitude and frequency. The effects of temperature were studied by setting a temperature gradient similar to that of real cable operation. The asymmetry of the physical parameters could seriously aggravate the accumulation of space charges in the AC field. A set of physical parameters based on these results was identified. Both the increase in voltage amplitude and decrease in frequency enhanced the amount and penetration into the insulation in the accumulated space charge. The dynamic behaviors of the space charges were more active with increased voltage amplitude and frequency. The temperature gradient in the cable insulation implies that the degree of accumulation, penetration into material, and activity of dynamic behaviors of the space charges at the warmest electrode are greater than those at the coldest. Compared with the DC field, the dynamic behavior of space charges in the AC electric field is more active and releases more energy. This research provides a theoretical basis for inhibiting the accumulation of space charges in an AC electric field.*

Keywords: ac electric field, cross-linked polyethylene, space charge, physical parameters, accumulation characteristics, dynamic behaviours

1. Introduction

Cross-linked polyethylene (XLPE) insulated cables are widely used in transmission and distribution systems of urban power grids owing to their excellent electrical properties. Under the long-term effects of electrical, thermal, and mechanical stresses, discharges may appear in XLPE insulation and ultimately break down, causing threats to the safety of the power grid. Electrical treeing is a common form of cable insulation failure, and many studies have shown that the dynamic behavior of space charges is a significant factor in the occurrence of aging through electrical treeing.[1,2] Space charges generated through injection at the electrodes or internal ionization led to the local electric field distortion upon accumulation. Moreover, the interaction of charges with the host material through trapping, detrapping, and recombination is accompanied by the release of energy, which may lead to irreversible changes in the chemical properties or physical structure of the polymer.[3] Therefore, it is necessary to investigate the dynamic behavior of space charges in cable insulation.

Since the invention of space charge measurement methods, space charge characteristics in insulating materials have been widely studied under direct current (DC) electric fields.[4-6] Parallel investigations under alternating current (AC) stress are rare because a net charge is not formed as easily as under DC stress, and the implementation of such tests with phase-resolved space charge patterns is more complex. With the development of phase-matching technology, some researchers have reported on the space charge accumulation function of the stressing time under AC. The evolution of the neat space charge as a function of aging time under an AC electric field was revealed by applying a method called all-phase averaging to eliminate the polarized charges that change with the voltage phase.[7-9] The accumulation of space charges under an AC field is lower than that existing under a DC field. However, in the long-term operation of the cable, the density of the space charges gradually increases, which may still affect the insulation performance of the cable. Currently, there is no

consensus on the mechanism of space charge accumulation under an AC electric field. Therefore, it is necessary to comprehensively investigate the factors influencing space charge accumulation under an AC electric field.

Polymer molecular bonds can be broken and reconstructed through energetic processes induced by the charges, representing a possible triggering step to electrical treeing.[10] Several studies have shown that the dynamic behavior of space charges is often accompanied by the release of energy.[2,11,12] Such energy exchanges, which can alter the chemical properties of polymer molecules and degrade the material, can occur near the interfaces during the injection and extraction of charges.[2] Additionally, the energy released by the recombination of charges near the two electrodes can cause electroluminescence and degrade the polymer.[11] The polarization energy released during repetitive charge trapping and detrapping could trigger degradation and electric treeing.[12] Therefore, it is necessary to explore the energy conversion during the dynamic transport of space charges. However, hitherto, only qualitative arguments have been primarily made; there appears to be a lack of quantitative approaches.

The charge transport processes are affected by the physical structure and chemical properties of the material, in addition to the voltage conditions and the operating environment of the cable. Actions on barrier height to injection, trap density, and trap energy substantially affect the charge migration.[13] The injection and migration of charges are closely related to the strength of the electric field, while processes such as trapping are not; there are also differences between the motion mechanisms of positive and negative charges. The presence of a temperature gradient and the nature of the electrode aradditional factors affecting the behavior of the cable insulation under operating DC stress.[14] These charge driving mechanisms in dielectrics also appear to play a role under AC stress. However, a comprehensive understanding of their influence is not available.

The dynamic behavior of space charges is complex; while the experimental measurement is able to aid the determination of the density change and position of neat space charge distributions, it cannot directly resolve the microscopic processes of generation and transport. To explore the dynamic transport process of space charges and the effect of charge interaction on charge accumulation, a simulation model must be established and compared with the experiments. A bipolar charge transport model was proposed by Alison and Hill[15], considering charge injection, migration, diffusion, trapping, detrapping, and recombination. The model was refined, and the influence of external conditions during operation under a temperature gradient and electric field gradient has been investigated.[16] A bipolar space charge transport model with different electric fields and temperatures can be used to simulate the real operation of the cable. However, in different studies, the charge parameters varied greatly. Therefore, it is necessary to explore the effects of different physical parameter values.

To sum up, one of the innovations of this paper is to set up asymmetrical physical parameters reasonably to make simulation and experiment consistent. On this basis, the quantitative analysis of charge density and energy density of trapping, detrapping, and recombination with different parameters and environmental conditions is another innovation of this paper. To achieve the above two points, a bipolar charge simulation model of an XLPE cable under an AC electric field was established. The effects of the physical parameters on the space charges dynamic behaviors are investigated by changing the mobility, injection barrier height, trapping coefficient, and detrapping barrier height. Moreover, the applicability of the model in an AC electric field was verified by comparing it with the experimental results. The dynamic transport process of space charges under different operating conditions of the cable was explored by changing the amplitude and frequency of the AC voltage. Finally, the effect of temperature on the dynamic behavior of the space charge is studied by setting the temperature gradient.

2. Space charge transport model

2.1 Transport mechanism of bipolar space charge transport model

The bipolar space charge transport model assumes that there are four types of charges in the insulating material. The exchange mechanisms that are considered herein are shown in Figure 1.

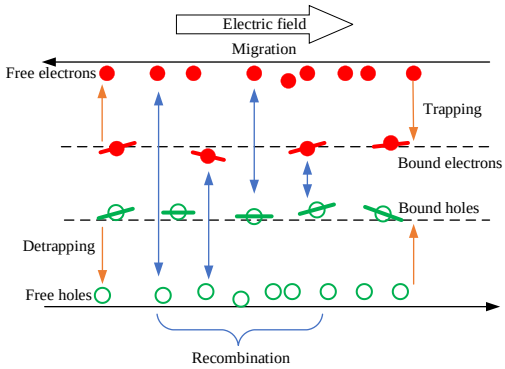

FIG.1. Elementary processes considered in the bipolar charge transport model.

The model assumes that the free electrons and free holes originate from the injection of two electrodes, ignoring the charge generated by the internal ionization of the material. The charge injection process follows the Schottky rule.[17]

$$J = AT^2\, exp(-\frac{\psi_{e,h}}{kT})\, exp(\frac{e}{kT}\sqrt{\frac{eE}{4\pi\varepsilon}}) \qquad (1)$$

where subscripts e and h refer to electrons and holes, respectively; A is the Richardson constant; T is the absolute temperature; e is the elementary charge; Ψ is the barrier height to injection; k is the Boltzmann constant; E is the electric field; and ε is the dielectric constant.

The charges need to overcome different potential barriers according to the electric field strength to be extracted,[17] as follows:

$$J_{oe} = -abs(-e\mu_e n_e E - D_e \nabla n_e) \quad (2)$$

$$J_{oh} = -abs(e\mu_h n_h E - D_h \nabla n_h) \quad (3)$$

Here, μ is the mobility, n is the charge density, and D is the diffusion coefficient. There is an Einstein relation between diffusion coefficient and mobility, as follows:

$$D_{e,h} = (kT/e)\mu_{e,h} \quad (4)$$

The physical or chemical defects that exist in polymer materials form many traps in the interior of the medium. Free charges can be trapped to become bound charges. Concurrently, bound charges are stimulated by thermal energy and detrapping. The dynamic behavior of the charges involving migration, diffusion, trapping, detrapping, and recombination in an insulating material can be described by the conduction equation, Poisson equation, and current continuity equation.[17]

Conduction equation:

$$J_{e/h} = \mu_{e/h} n_{e/h}(x,t) E(x,t) = v_{e/h} n_{e/h} \quad (5)$$

Poisson equation:

$$\nabla^2 V = \frac{\partial^2 V(x,t)}{\partial x^2} = -\frac{\rho(x,t)}{\varepsilon} \quad (6)$$

$$E = -\nabla V \quad (7)$$

Current continuity equation:

$$\frac{\partial n_a(x,t)}{\partial t} + \frac{\partial J_a(x,t)}{\partial x} = s_a(x,t) \quad (8)$$

Here, ρ(x) is the net charge density of four types of space charges at position x; J_a is the current density of free electrons and holes; μ is the mobility of the free charges; ν is the velocity of free charges; and n_a is the density of a given type of charge.

Now, s_a on the right side of Equation (8) is the source term, meaning that, excluding the density changes caused by the injection, migration, and extraction of space charges, only the density changes caused by the recombination, trapping, and detrapping of space charges are considered. The details are as follows.

$$s_e = -R_{eh} n_e n_h - R_{eht} n_e n_{ht} - T_e n_e \left(1 - \frac{n_{et}}{n_{0et}}\right) + v\, exp\left(\frac{-\psi_{et}}{kT}\right) n_{et} \frac{n_{et}}{n_{0et}} \quad (9)$$

$$s_h = -R_{eh} n_e n_h - R_{eht} n_e n_h - T_h n_h \left(1 - \frac{n_{ht}}{n_{0ht}}\right) + v\, exp\left(\frac{-\psi_{ht}}{kT}\right) n_{ht} \frac{n_{ht}}{n_{0ht}} \quad (10)$$

$$s_{et} = -R_{eht} n_{et} n_h - R_{etht} n_{et} n_{ht} + T_e n_e \left(1 - \frac{n_{et}}{n_{0et}}\right) - v\, exp\left(\frac{-\psi_{et}}{kT}\right) n_{et} \frac{n_{et}}{n_{0et}} \quad (11)$$

$$s_{ht} = -R_{eht} n_e n_{ht} - R_{etht} n_{et} n_{ht} + T_h n_h \left(1 - \frac{n_{ht}}{n_{0ht}}\right) - v\, exp\left(\frac{-\psi_{ht}}{kT}\right) n_{ht} \frac{n_{ht}}{n_{0ht}} \quad (12)$$

where s_e, s_h, s_{et}, and s_{ht} are the change rates of the density of four kinds of charges, respectively, caused by recombination, trapping, and detrapping. Moreover, n_e, n_h, n_{et}, and n_{ht} are the densities of the four kinds of charges, respectively; R is the recombination coefficient between the charges; n_{0et} and n_{0ht} are the deep trap densities of the electrons and holes, respectively; T_e and T_h are the electron and hole trapping coefficients, respectively; v is the detrapping rate; Ψ_{et} and Ψ_{ht} are the barrier heights of the bound electrons and holes, respectively.

2.2 Parameters setting and simulation conditions

The values of the recombination coefficient, trap density, and detrapping rate are consistent in most literatures.[18-21] However, the values of injection barrier height, detrapping barrier height, mobility, and trapping coefficient are quite different in different studies. These four parameters are related to the physical structure and chemical properties of the material. However, the processing technology, aging degree, trap, air gap, impurities, and other factors will affect the test results of the parameters. Therefore, only a relatively reasonable value range of these four parameters can be obtained through experimental tests, and it is difficult to obtain accurate values. In different simulation studies, the values of these four parameters differ greatly. Some of these parameters even differ by orders of magnitude. According to previous studies, the value range of each parameter can be obtained. The injection barrier height ranges from 1.1 eV to 1.27 eV.[18-24] The detrapping barrier height is in the range of 0.90 eV to 0.99 eV.[18-20.22-24] The magnitude range of the mobility value is 10^{-16} $m^2V^{-1}s^{-1}$ to 10^{-12} $m^2V^{-1}s^{-1}$.[15,18-23,25] The trapping coefficient ranges from 0.007 s^{-1} to 0.2 s^{-1}.[15,18-24] Reasonable values taken from these ranges are listed in Table 1, and are considered as default values.

The XLPE insulation sample slice of 230 μm thickness was resolved as a one-dimensional simulation model using finite element software. The grounding point was at 0 μm, and the sinusoidal AC voltage was applied at 230 μm: $V(t) = V_0 \sin(2\pi f t)$. The considered peak voltage is V0 = 8.0 kV and the frequency is f = 50 Hz. The temperature was 293 K. The model was resolved after 60 min of voltage application.

Table 1. Setting of symmetrical parameters used in the simulations.

Parameters	Values
$\psi_{e,h}$ (Injection barrier height)	1.2 eV
$\psi_{et,ht}$ (Detrapping barrier height)	0.97 eV
$\mu_{e,h}$ (Mobility)	2×10^{-12} $m^2V^{-1}s^{-1}$
$T_{e,h}$(Trapping coefficient)	0.1 s^{-1}
$R_{eht,eth,etht}$(Recombination coefficient for other than between free electrons/holes)	4×10^{-3} $m^3C^{-1}s^{-1}$
$R_{e,h}$(Recombination coefficient between free charges)	0
$n_{0et,0ht}$(Trap density)	5.9×10^{20} m^{-3}
$D_{e,h}$(Diffusion coefficient)	5.05×10^{-14} m^2/s
υ (Detrapping rate)	6×10^{12} s^{-1}
ε_r (Relative permittivity)	2.3

3. Influence of physical parameters on the dynamic behavior of space charge

3.1 Dynamic behavior of space charges with symmetrical parameters

A bipolar space charge transmission model with symmetrical parameters under the AC electrical field was calculated, and the curve of the space charge density at the phase of 0° within 60 min was obtained, as shown in Figure 2. When the model parameters are symmetrical, there is no apparent accumulation of space charges under the AC field. The space charge density at the two electrodes remains extremely low, at approximately 1.1×10^{-3} C/m³, and does not increase gradually with time. Take the upper electrode (230um) as an example. Positive charges are injected during the positive half-wave, while negative charges are injected during the negative half-wave, and positive and negative charges will recombine. When the physical parameters of positive and negative charges are equal, the densities of positive and negative charges are equal, so the two almost completely recombine and it is difficult to accumulate. But this is not consistent with the phenomenon of the space charge accumulation measured experimentally. Space charge will accumulate slowly under the AC field, which is consistent with the actual situation of cable. In order to explore the reason why the space charges with symmetrical parameters do not accumulate, the space charge densities of trapping, detrapping, and recombination were quantitatively analyzed.

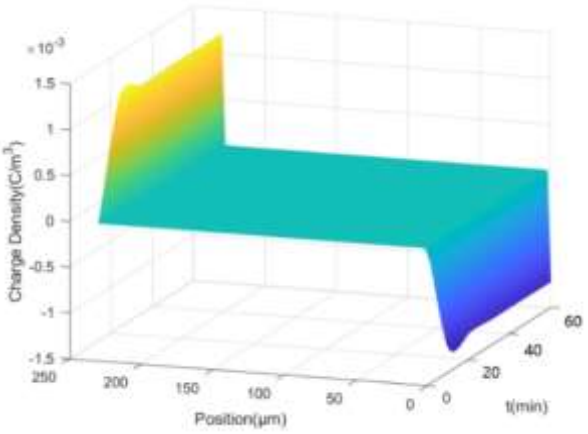

FIG. 2. Accumulation of space charges with symmetrical parameters at a phase of 0° within 60 min of stressing.

The space charge densities of trapping, detrapping, and recombination in an AC cycle are shown in Figure 3. The quantities that are plotted represent the total charge involved in the processes for one period of the AC stress, which is calculated by integrating the rate of behaviors, using the following equations, and the Figure 13、Figure 20、Figure 22，and Figure 23 are also derived from these.

$$n_{trapping} = \sum \int T_{e/h} n_{e/h} \left(1 - \frac{n_{et/ht}}{n_{0et/0ht}}\right) dt \quad (13)$$

$$n_{de-trapping} = \sum \int v\, exp(\frac{-\psi_{et/ht}}{kT}) n_{et/ht} \frac{n_{et/ht}}{n_{0et/0ht}} dt \quad (14)$$

$$n_{recombination} = \sum \int R_{eh/eht/eth/etht} n_{e/h/et/ht} n_{e/h/et/ht}\, dt \quad (15)$$

The space charge processes are more active near the electrodes, while the space charge density is almost zero in the middle of the material. The maximum space charge density involved in trapping near the electrode interface is 9.9×10^{-6} C/m³. Moreover, the space charge density involved in detrapping is three orders of magnitude lower; meanwhile, the space charge density involved in recombination is 1.17×10^{-5}C/m³, which is slightly higher than that of trapping. This is because, besides the bound charges, fewer free charges recombine with the bound charges with opposite polarity.

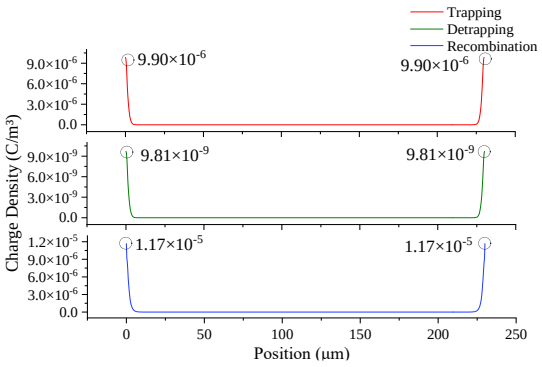

FIG. 3. Space charge densities involved in trapping, detrapping, and recombination in a voltage cycle (0.02 s) within 60 min with symmetrical parameters.

As shown in Figure 3, a few bound charges are detrapped, and most of them disappear through recombination. Therefore, an important reason for the non-accumulation of space charges with symmetrical parameters is that the space charges injected in the positive half wave of voltage are extracted or recombined in the negative half wave of voltage. However, several studies have found that the movement mechanisms of positive and negative space charges are different.[20-23] Specifically, the efficiency of injection, trapping, detrapping, and the migration speed are not exactly identical, which may lead to a remnant of space charge in the insulation after a period of voltage application. This is an important reason for the accumulation of space charge during the long-term operation of the cable. Therefore, to explore the influence of asymmetrical physical parameters on space charge accumulation, it is necessary to set the injection barrier, mobility, trapping coefficient, and detrapping barrier of positive charges apart from those of negative charges.

3.2 Influence of the asymmetry of physical parameters on the dynamic behavior of space charges

The influence of each parameter on charge dynamic behavior is judged from two aspects. The first is the process of charge accumulation, as shown in Figure 4, 6, 8 and 10. The other is maximum space charge density of trapping, detrapping, and recombination in the direction of thickness

in one voltage period (0.02 s) after 60 min of applying voltage, as shown in Figure 5, 7, 9 and 11.

3.2.1 Injection barrier.

The injection barrier determines the efficiency of the free electron and hole injection from the electrodes. Here, the injection barrier of the free electrons is maintained as 1.2 eV, while that of the free holes is set as 1.19 or 1.21 eV. The other parameters, voltage, and simulation conditions were the same as those of the symmetrical model. The accumulation process of the space charge within 60 min is shown in Figure 4. When the injection barrier of the free holes was lower than that of the free electrons, positive charges accumulated at the two electrodes. When the injection barrier of the free holes was higher than that of the free electrons, negative charges accumulated. This was because space charges with a relatively lower injection barrier were more easily injected into the material.

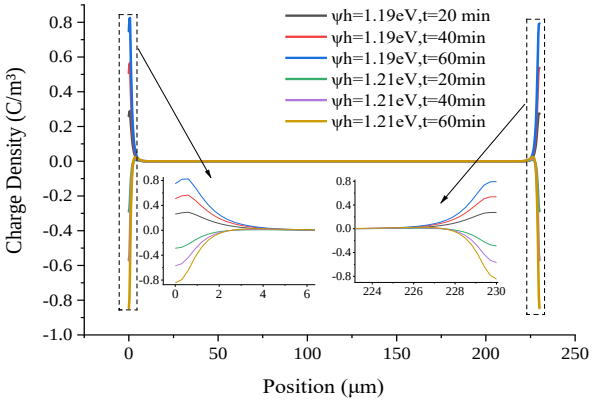

FIG. 4. Space charge profiles for a phase of 90° as a function of time of voltage application for an injection barrier of free electrons of 1.2 eV and injection barrier of free holes of 1.19 or 1.21 eV.

As the injection barrier of the free holes increased, the density of the space charge involved in trapping and recombination decreased owing to the decrease in the injected charge amount, as shown in Figure 5. The asymmetry of the injection barriers led to a decrease in the detrapping charge density. When the injection barrier of the free holes was at its highest level, the space charge density of the detrapping was the lowest.

3.2.2 Mobility.

Mobility mainly affects the migration of free charges in the material. The mobility of free electrons is maintained at 2×10^{-12} $m^2V^{-1}s^{-1}$, while that of free holes is set as 1×10^{-12} or 3×10^{-12} $m^2V^{-1}s^{-1}$. The other parameters and voltage conditions remained unchanged. The accumulation process of the space charge within 60 min is shown in Figure 6. When the mobility of free holes was lower than that of free electrons, positive charges accumulated near the electrode interface, and the negative charges accumulated at 4–8 μm from the electrodes. For higher hole mobilities for electrons, negative charges accumulate near the electrode interface, and positive charges accumulate deep in the materials. This is because the space charges with higher mobility can migrate deeper into the material and offer a lower probability of being recombined, resulting in the accumulation of space charges with higher mobility at the depth of the material.

The asymmetry in the mobility of the positive and negative free charges decreased the space charge densities of trapping and recombination, as shown in Figure 7. When the mobility of free holes was at its maximum, the space charge densities of trapping and recombination were at their minimum levels. The space charge of trapping decreased with an increase in the mobility of free holes.

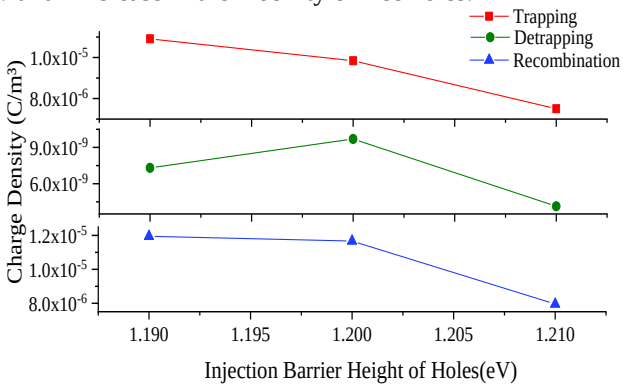

FIG. 5. Relationship between the maximum space charge density of trapping, detrapping, and recombination in the direction of thickness and the injection barrier of free holes in one voltage period (0.02 s) after 60 min of applying voltage.

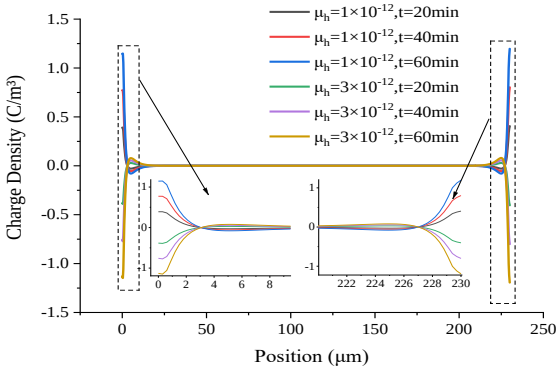

FIG. 6. Space charge density profiles for mobility of free electrons of 2×10^{-12} $m^2V^{-1}s^{-1}$ and mobility of free holes of 1×10^{-12} or 3×10^{-12} $m^2V^{-1}s^{-1}$.

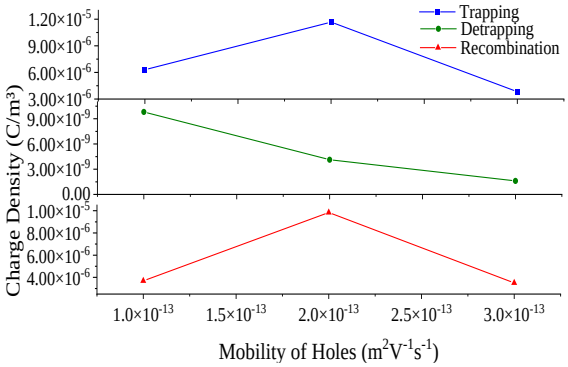

FIG. 7. Relationship between the space charge density of trapping, detrapping, and recombination in the direction of thickness and the mobility of free holes in one voltage period (0.02 s) after 60 min of applying voltage.

3.2.3 Trapping coefficient.

The trapping coefficient reflects the ability of traps to capture free charges. The trapping coefficient of the free electrons is maintained at 0.1 s^{-1}, while that of the free hole is set as 0.05 and 0.15 s^{-1}. The other parameters are set to default values. The accumulation of space charges within 60 min is shown in Figure 8. When the trapping coefficient of the free electrons is greater than that of the free holes, negative charges accumulate at the two electrodes. When the trapping coefficient of the free electrons is lower than that of the free holes, positive charges accumulate at the two electrodes. Charges with a higher trapping coefficient are more likely to be captured by the traps near the electrodes, limiting migration to the interior of the material.

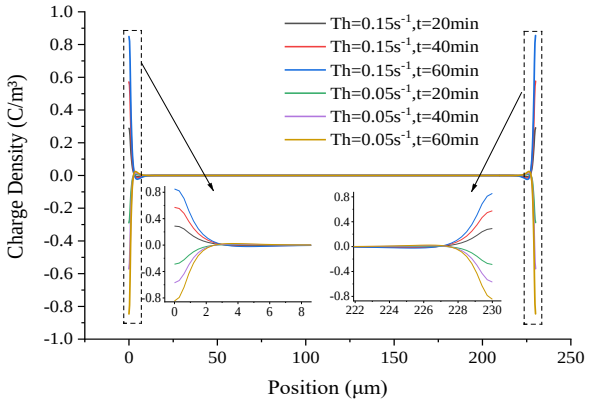

FIG. 8. Space charge density profiles with trapping coefficient of free electrons of 0.1 s^{-1} and trapping coefficient of free holes of 0.05 or 0.15 s^{-1}.

As the hole trapping coefficient increased, the space charge density of trapping and recombination increased, as shown in Figure 9. More free charges were captured by the traps after being injected and recombined with charges of opposite polarity. The asymmetry between the trapping coefficients of the free electrons and holes increased the space charge density of detrapping. When the trapping coefficient of the free holes was at its highest, the space charge density of detrapping was similarly at its highest.

3.2.4 Detrapping barrier height.

The detrapping barrier heights are the depths of the traps that can capture free charges. It represents the energy needed for the bound carriers to escape the traps when they are occupied. The detrapping barrier height of the bound electrons was set as 0.97 eV, and that of the bound holes was set as 0.95 or 0.99 eV. The other parameters remained unchanged. The accumulation of charges within 60 min is shown in Figure 10. The positive charge density decreased, and the negative charge density increased near the two electrodes with a decrease in the detrapping barrier of the bound holes. This was because charges with a higher detrapping barrier have more difficulty in escaping from the traps. Therefore, when the charges are injected from the electrodes and captured by the traps, the charges with a lower detrapping barrier are able to escape easily and migrate internally; meanwhile, the charges with higher detrapping barriers are captured near the electrodes and gradually accumulate. However, owing to the relatively small number of charges that are excited, the asymmetry of the detrapping barrier heights has a relatively low effect on the neat charge accumulation. The asymmetry of the detrapping barrier heights leads to a decrease in the space charge density of trapping and recombination, as shown in Figure 11. The space charge density decreased with an increase in the detrapping barrier height of the bound holes.

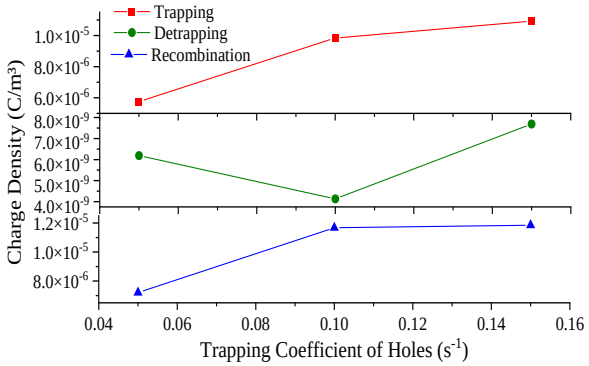

FIG. 9. Relationship between the space charge density of trapping, detrapping, and recombination in the direction of thickness and the trapping coefficient of free holes in one period (0.02s) after 60 min of applying voltage.

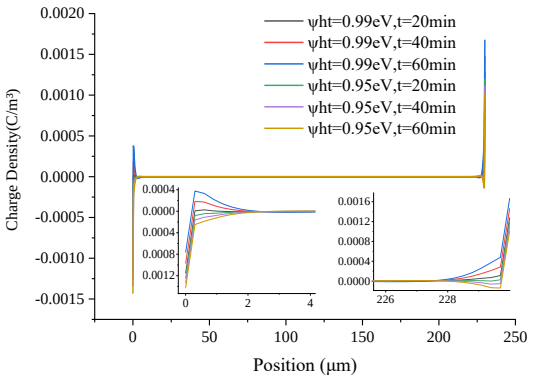

FIG. 10. Space charge density profiles with detrapping barrier height of free electrons of 0.97 eV and that of free holes of 0.95 or 0.99 eV.

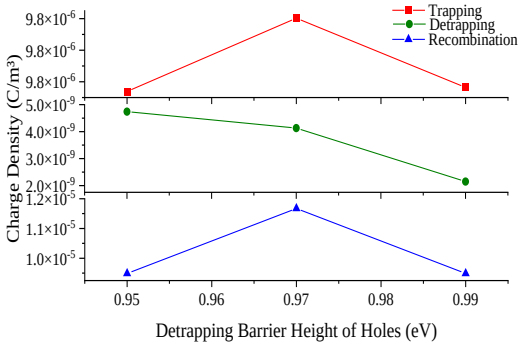

FIG. 11. Relationship between the space charge density of trapping, detrapping, and recombination in the direction of thickness and the detrapping barrier height of free holes in one period after 60 min of applying voltage.

3.3 Dynamic behavior of space charges with fully asymmetric physical parameters

The asymmetry of physical parameters, such as the injected barrier, mobility, trapping coefficient, and detrapping barrier of space charges, led to differences in density, migration velocity, trapping, and detrapping density of positive and negative space charges. The mechanism of space charge accumulation under an AC field was the cause of the interaction of multiple physical parameters. Therefore, it was necessary to set multiple asymmetrical physical parameters simultaneously. Referring to the simulation study of asymmetrical parameters in the DC electric field and the experimental results in the AC electric field, the asymmetrical parameters of space charges were set as shown in Table 2.[26-31] Other parameters remain unchanged.

Table 2. Setting of asymmetrical parameters.

Parameters	Value
$\psi_{e,h}/eV$ (Injection barrier height)	1.19, 1.21
$\psi_{et,ht}/eV$ (Detrapping barrier height)	0.95, 0.97
$\mu_{e,h}/(m^2V^{-1}s^{-1})$ (Mobility)	3×10^{-12}, 1×10^{-12}
$T_{e,h}/(s^{-1})$ (Trapping coefficient)	0.05, 0.1

The accumulation of space charges within 60 min with asymmetrical parameters is shown in Figure 12. The positive space charges gradually accumulated near the electrode interface (0–1 μm), while the negative space charges gradually increased with time in the insulation (1–8 μm). Compared with the symmetrical parameters, the space charge densities of trapping, detrapping, and recombination all decreased, as shown in Figure 13.

In particular, the charge density of recombination was 2.92×10^{-6} C/m³, which was slightly lower than that of trapping. This indicates that some of the bound charges did not participate in the recombination, but remained in the insulation, which is an important reason for the accumulation of space charge under asymmetrical parameters.

To verify the reliability and applicability of the model with asymmetrical parameters, it is necessary to compare the simulation with the experimental results. The space charge measurement method under AC electric field has already been reported in our past work[32] and only a brief outline is given here. In order to ensure that the conditions of the experiment and simulation are consistent so that the experimental and simulation results are comparable, the XLPE cable insulation was cut into samples with a thickness of 230 μm and an area of 45 × 45 mm². An AC electric field of 50 Hz and 35 kV/mm (RMS value) was then applied to the slices for 6 h. The space charges were measured through the space charge measurement system based on the pulsed electro-acoustic method (PEA). Then the results were processed using the all-phase average method to filter out the interface polarization charges that change periodically with the voltage phase. The remainder is the gradually accumulating space charge injected by the electrodes.

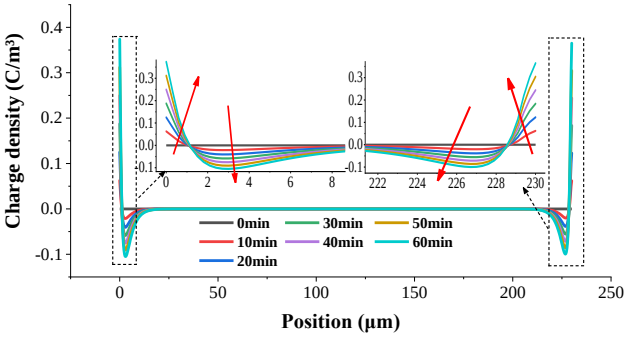

FIG. 12. Accumulation of space charges with asymmetrical parameters within 60 min calculated by simulation.

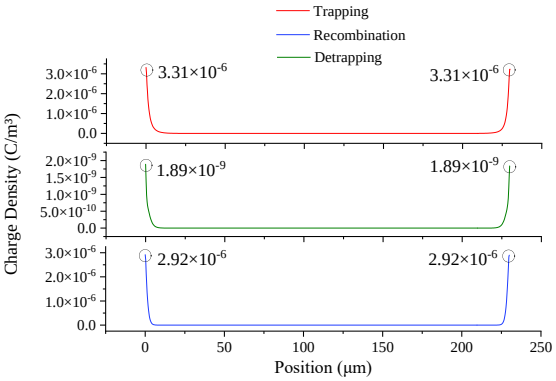

FIG. 13. Space charge densities of trapping, detrapping, and recombination in a voltage cycle (0.02 s) within 60 min with asymmetrical parameters calculated by simulation.

The obtained accumulation rule of the space charges in the AC field is shown in Figure 14. As the upper electrode (230um) is far from the piezoelectric sensor used to measure the signal, the signal attenuated. The positive charges at the upper electrode (230um) are difficult to be fully restored. But the presence of positive charges can still be seen from the far right of Figure 14. In addition, the charge accumulation distribution of the upper electrode and the lower electrode is symmetrical under the AC electric field theoretically, so the charge accumulation of the upper electrode (230um) can be obtained through the charge distribution of the lower electrode (0um).

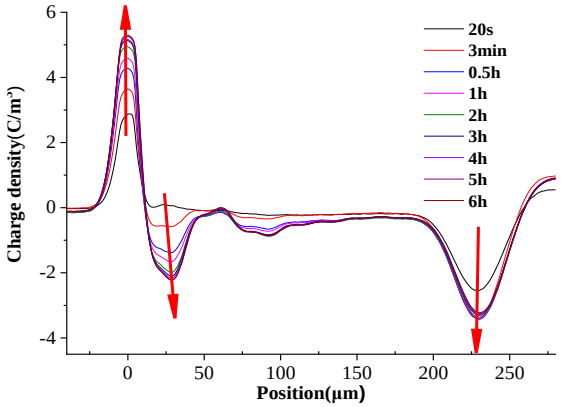

FIG. 14. Accumulation process of space charges within 6 h measured by experiment.

That is, the positive charges accumulate near the two electrodes, while the negative charges accumulate slightly away from the electrodes. Although the simulation time was shorter than the experimental measurement time and the simulated space charge density was lower, the accumulation rules of positive and negative charges were consistent. It can be predicted that, when the simulation time is extended, the amount of space charges will increase, and the distance into the insulation will deepen gradually. Therefore, by comparing the simulation and experiment, it can be verified that the model with asymmetrical parameters is reasonable and feasible.

4. Influence of voltage conditions on the dynamic behavior of space charges

The amplitude and frequency of the AC voltage affect the injection, extraction, migration speed, and distance of space charges. The voltage amplitude evidently affects the amount of injected charges and their velocity. Changing the frequency will affect the number of stress periods as well as the drift time for charges in one period. The analysis of these effects is based on the model with asymmetrical parameters. Figure 15 shows the accumulation of space charge for 60 min with different amplitudes of AC voltage. The voltage frequency remained at 50 Hz. As the peak voltage rose from 6.0 to 8.0 kV, and subsequently, to 10.0 kV, the maximum density of positive space charges rose from 0.17 to 0.37 C/m³, and finally, to 0.54 C/m³. The maximum density of negative space charges increased from 0.05 to 0.1 C/m³, and finally, to 0.13 C/m³. The distance of the space charges into the material increased from 10 to 18 μm, and finally, to 26 μm. Finally, the increase in voltage amplitude enhanced the charge velocity and the accumulation distance into the material.

Figure 16 shows the relationship between the dynamic behavior of the space charges and the voltage amplitude. With the increase in voltage amplitude, the space charge densities of trapping, detrapping, and recombination increased almost linearly because of a larger amount of injected charges.

Figure 17 shows the accumulation of space charges with different AC voltage frequencies within 60 min. The voltage amplitude remained at 8.0 kV. Figure 17 shows that, as the voltage frequency rises from 40 to 50 Hz, and then, to 60 Hz, the maximum density of positive space charges dropped from 0.39 to 0.37 C/m³, and finally, to 0.31 C/m³. The maximum density of negative space charges dropped from 0.11 to 0.1 C/m³, and then, to 0.08 C/m³. The distance of the space charges into the material decreased from 25 to 18 μm, and finally, to 12 μm. Meanwhile, the increase in the voltage frequency attenuated the accumulation and distance into the material of space charges. The change in the charge density of trapping, detrapping, and recombination increases with frequency, as shown in Figure 18. But this change is nonlinear, the higher the frequency, the greater the impact of the change in frequency.

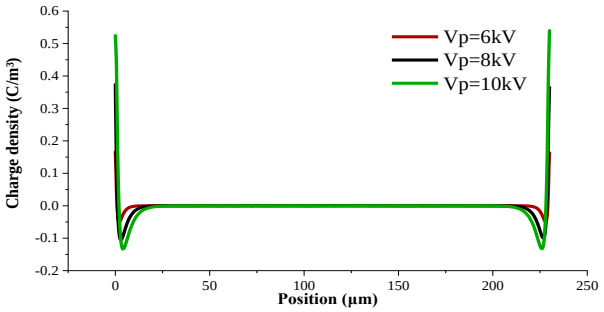

FIG. 15. Accumulation of space charge within 60 min with different AC voltage amplitudes.

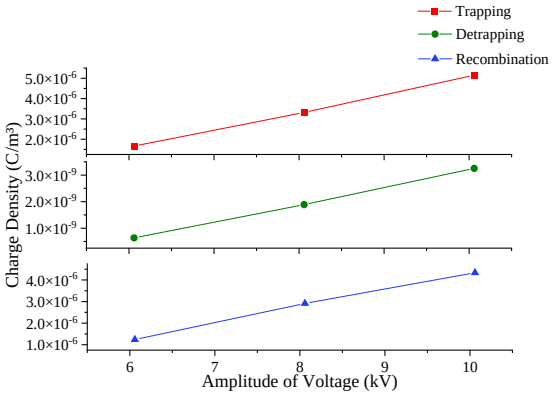

FIG. 16. Relationship between maximum space charge density of trapping, detrapping, and recombination in the direction of thickness and voltage amplitude in a voltage cycle (0.02 s) after 60 min of applying voltage with asymmetric parameters.

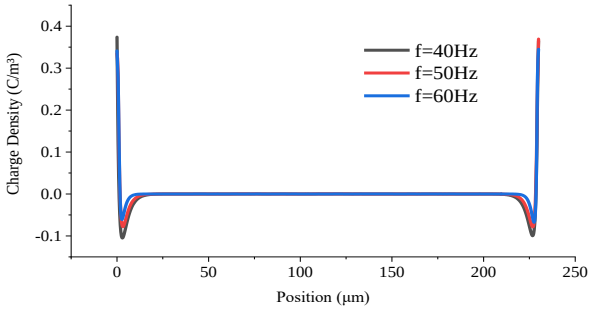

FIG. 17. Accumulation of space charge within 60 min with different AC voltage frequencies.

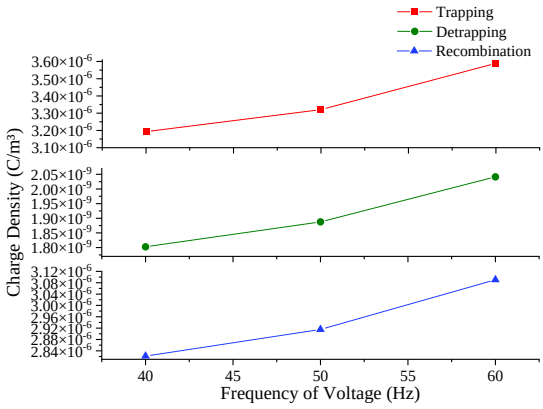

FIG. 18. Relationship between the maximum space charge density of trapping, detrapping, and recombination in the direction of thickness and voltage frequency in 0.02 s after 60 min of applying voltage with asymmetric parameters.

With the increase of frequency, though the charge accumulation decreases, the charge dynamic behaviors become more active. In the insulation medium of AC cables, the charge accumulation is small, but the alternating direction of the electric field leads to active charge dynamic behaviors. Therefore, the charge dynamic behavior accompanied by energy release plays a dominant role in the insulation deterioration of AC cables. Hence, more active charge behavior is one of the important reasons for insulation deterioration under high frequency conditions.

5. Influence of temperature gradient on dynamic behavior of space charges

When the high-voltage cable is in normal operation, the conductor temperature is higher than the ambient temperature of the cable, owing to Joule losses. Hence, the insulation was subjected to a temperature gradient. To account for this feature, the temperature of the high-voltage electrode (at a position of 230 μm) was set at 303 K, and that of the ground electrode (0 μm) was set at 293 K. The bipolar charge model was resolved under this temperature gradient, and the accumulation process and distribution of space charges in the insulation within 60 min were obtained, as shown in Figure 19. The amount of accumulated charge and their distance into the material at the high-voltage electrode were much greater than those at the ground electrode. This was because the higher temperature intensified the dynamic processes of charge injection and migration, which increased the degree of space charge accumulation. Notably, in the model considered here, the two processes (injection and detrapping) are temperature dependent, while the trapping and recombination coefficients are temperature independent.

Figure 20 shows the space charge density profiles under this temperature gradient. The charge amount involved in trapping, detrapping, and recombination at the higher temperature electrode was much higher than that of the colder electrode. Moreover, the space charges involved in recombination were less than those involved in trapping, leading to the accumulation of bound charges. Therefore, an increase in temperature will increase the activity of the space charge dynamic behavior.

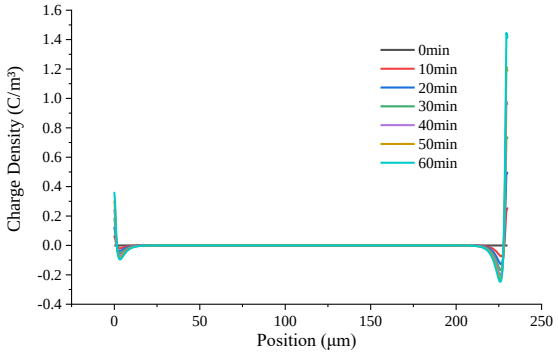

FIG. 19. Accumulation process of space charges under temperature gradient within 60 min.

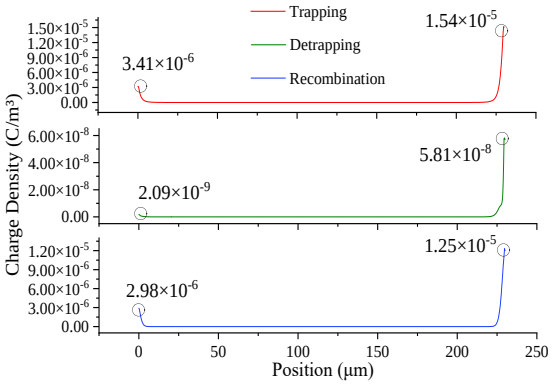

FIG. 20. Space charge density of trapping, detrapping, and recombination in one voltage cycle within 60 min under temperature gradient.

6. Discussion

6.1 Field distortion in the insulation

The accumulation of space charges led to a serious local electric field distortion in the polymer. An extremely high electric field can trigger the growth of structural defects, followed by partial discharges and failure. Therefore, we focused on the effect of charge accumulation on the local electric field distortion.

We consider the space charge data obtained with asymmetrical parameters, as shown in Figure 12. The peak value of the AC field was 35 kV/mm, and the frequency was 50 Hz. When the amplitude of the applied voltage was zero, that is, when the intensity of the applied electric field was zero, the accumulated positive and negative charges generated an additional electric field inside the insulating material, for a stress time of 60 min, as shown in Figure 21(a). The maximum value of the additional electric field was 2.96×10^4 V/m, and the additional electric field at the two electrodes is in opposite directions, pointing to the interior of the insulation from the electrode interface.

Depending on the phase of the AC stress, the additional electric field either strengthens or weakens the total field. The electric field at the ground electrode (cathode) was weakened in positive half wave, while that which was found at the high voltage electrode (anode) was enhanced, as shown in Figure 21(b). The situation was reversed in the negative half wave, as shown in Figure 21(c).

As the stressing time increased, the accumulated space charge gradually increased, such that the distortion degree of the electric field also increased. When the local electric field exceeds a certain threshold, irreversible damage, such as partial discharge or electric trees inside the medium, will be produced. Moreover, the enhancement of the local electric field will affect the dynamic behavior of the charges in the materials, such as injection and migration, strengthen the collision by free electrons, and possibly produce ionization. As a side effect, an increase in the temperature of the medium may occur, which will have a detrimental effect on the insulation properties of materials. For these subsequent

processes, the energetic aspects of charge exchange need to be considered.

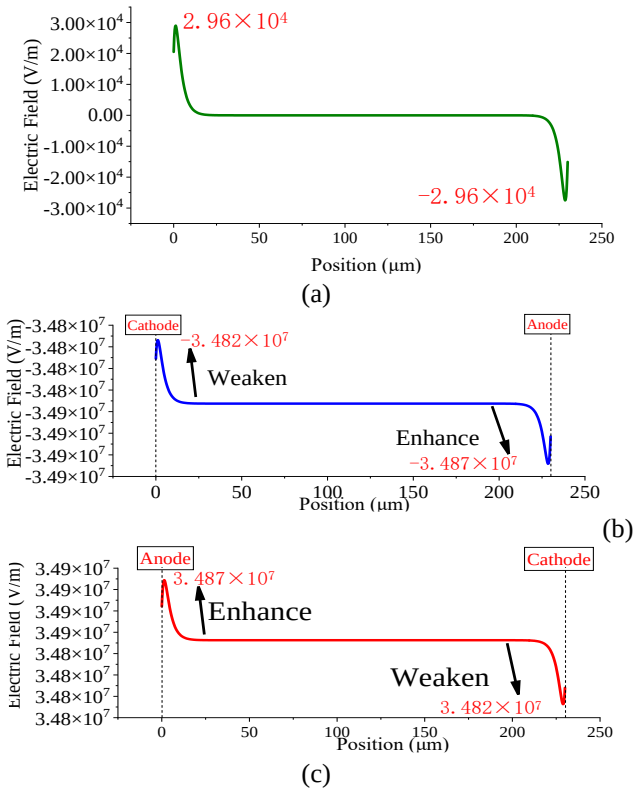

FIG. 21. Electric field profiles at different phases of the AC stress, accounting for the space charge effect. (a) Zero crossing point. (b) Positive half wave of AC voltage (ωt=90°). (c) Negative half wave of AC voltage (ωt=270°).

6.2 Energetic aspects of the dynamic behavior on insulation

The shallow trap energy levels of insulating polymeric materials generally exist as Anderson localized states, that is, near the conduction and valence bands. This corresponds to a physical disorder of the material. The transport of free charges mostly occurs through these localized states.[24]

Deeper trapping centers generally involve chemical defects. When a free electron is trapped as a bound charge, it releases an energy of less than 1.5 eV.[3] The bound charge will generate an additional electric field, which will cause the surrounding charge to be polarized and deepen the depth of the trap to approximately 2–5 eV. [3] This energy is stored in the form of electromechanical energy, which is released when the bound electrons detrap and the polarization disappears. The energies released by the trapping and detrapping of holes are similar to those of electrons.

In contrast to trapping and detrapping, recombination is a process that releases a considerable amount of energy. The recombination process between the bound electron and hole is specific. The bound electron first stabilizes in an excited state at the recombination center, and then, decays to the ground state when interacting with the positive charge.[3] The energy released in this process is greater than 5 eV[3], and is usually in the form of photons.

The energies that were released in the process of charge trapping, detrapping, and recombination were quantitatively calculated. It is assumed that the minimum energy released by each event of charge trapping, detrapping, and recombination is 1.5, 2, and 5 eV, respectively. In the model with asymmetrical parameters with the peak amplitude of 8kV and the frequency of 50 Hz, the energies released by space charge dynamic behavior in an AC cycle (0.02 s) after 60 min of field application are shown in Figure 22. In one voltage period, the total energy released by space charge trapping is 3.11×10^{13} eV/m³, the energy released by detrapping is 2.36×10^{10} eV/m³, and the energy released by recombination is 9.10×10^{13} eV/m³.

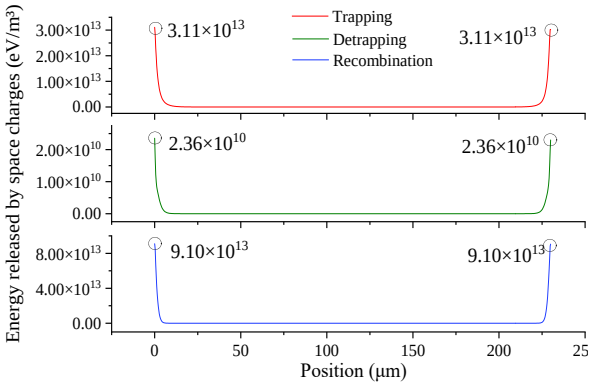

FIG. 22. Energy released by space charge trapping, detrapping, and recombination in an AC cycle (0.02 s) after 60 min of stressing under AC voltage of 8kV(peak value).

The dissociation energy of most chemical bonds in XLPE is 4–5 eV. A significant amount of energy is released in the dynamic behavior of space charges, and converted into different forms, such as phonons. In particular, the energy released in the recombination process causes electroluminescence, which may constitute a fingerprint of the damage to the structure of the polymer molecular chain. For comparison purposes, the energy released by space charges in 0.02 s under the DC electric field is shown in Figure 23.

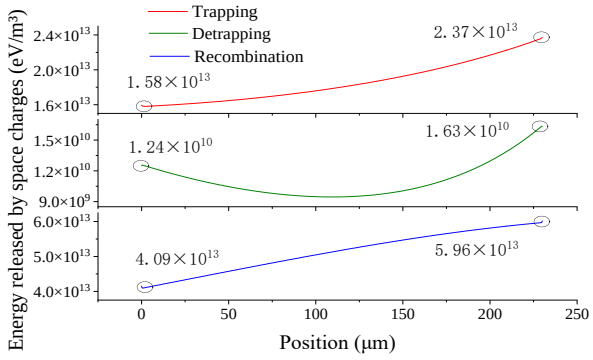

FIG. 23. Energy released by space charge trapping, detrapping, and recombination within 0.02 s after 60 min of stressing under DC votage of 8 kV.

Notably, the DC and AC peak electric field strengths were the same. Compared with the DC electric field, the energy released by the space charge of trapping, detrapping, and recombination in the AC electric field was approximately twice as much as that in the DC electric field, while the RMS AC field was 30% less than that of the DC field. This is because the alternating voltage polarity intensifies the activity of space charge behaviors, especially recombination. This will seriously affect the insulation characteristics of AC cables, which is an important reason for aging through electric treeing.

7. Conclusions

A bipolar space charge transport model under an AC field was established and solved. By changing the physical parameters, voltage conditions, and setting the temperature gradient, the factors influencing space charge dynamics were studied. The feasibility of parameter selection was verified by comparison with various experiments. The distortion of the local electric field caused by the accumulation of space charges and the energy released dynamically by space charges were discussed.

The asymmetry of the injection barriers, mobilities, trapping coefficients, and detrapping barriers led to differences in the motion and accumulation of positive and negative space charges. In comparison with experimental results, a set of asymmetrical physical parameters that are consistent with the experimental results were obtained. The asymmetry of physical parameters results in the accumulation of positive charges near the electrode interface and negative charges in the deeper insulation.

Based on the asymmetric parameter simulation model, the peak value and frequency of the AC voltage were changed, and the temperature gradient was set. The degree of space charge accumulation and the distance into the insulation increased with an increase in the voltage peak and decreased with an increase in frequency. The densities of charge, involved in trapping, detrapping, and recombination, increased linearly with the increase in amplitude but increased nonlinearly with the frequency. The temperature gradient resulted in the amplitude of space charge accumulation, and the distance of space charge into the material at the warmer electrode was much greater than that at the colder electrode. Furthermore, the dynamic behavior of the space charge at the warmer electrode was more active than that of the lower electrode.

The space charge accumulation forms an additional electric field near the two electrodes, which is directed from the electrode interface to the interior of the insulation, and weakens the cathode electric field, while strengthening the anode electric field. Compared to trapping and detrapping, space charge recombination releases more energy and has a more serious effect on insulation. The energy released by space charges under an AC electric field is more than twice that under a DC electric field. Even if the space charge accumulation is less under the AC electric field, the influence of the energy released by space charge dynamic behaviors on the destruction of the molecular chain structure cannot be ignored. This study provides theoretical guidance for improving the performance of cable insulation from a micro point of view.

Acknowledgments

This research was financed by the Shandong Provincial Natural Science Foundation (Grant No. ZR2019QEE013) and the National Natural Science Foundation of China (Grant No.51907105 and No. U1966209).

Data availability statement

The data that support the findings of this study are available upon reasonable request from the authors.

References

[1] Montanari G. C. 2011 *IEEE Transactions on Dielectrics and Electrical Insulation* **18** 339

[2] Xie A. S., Li S. T., Zheng X. Q. and Chen G. 2009 *Journal of Physics D: Applied Physics* 42 125106

[3] Laurent C., Teyssedre G., Roy Le S., and Baudoin F. 2013 *IEEE Transactions on Dielectrics and Electrical Insulation* **20** 357

[4] Zheng Y., Huang H., Zhong X. and Serdyuk Y. V 2021 *Journal of Physics D: Applied Physics* **54** 235501

[5] Beldjilali A., Saidi-Amroun N., and Saidi M. 2016 *Tansactions on Dielectrics and Electrical Insulation* **23** 573

[6] Matsui K., Tanaka Y., Takada T., Fukao T., Fukunaga K., Maeno T., and Alison J. M. 2005 *IEEE Transactions on Dielectrics and Electrical Insulation* **12** 406

[7] Thomas C., Teyssedre G., and Laurent C. 2010 *Journal of Physics D: Applied Physics* **44**, 015401

[8] Thomas C., Teyssedre G., and Laurent C. 2008 *IEEE Transactions on Dielectrics and Electrical Insulation* **15**, 554

[9] He D, Wang W., Li J., Teyssedre G., and Laurent C. 2016 *IEEE Transactions on Dielectrics and Electrical Insulation* **23** 2404

[10] Zhang Y. X., Zhou Y. X., Wu C.,Zhang L., Teng C. Y., and Nie H. 2020 *Journal of Physics D: Applied Physics* **53** 415501

[11] Baudoin F., Mills D. H., Lewin P. L., Roy Le S., Teyssedre G. and Laurent C. 2011 *Journal of Physics D: Applied Physics* **44** 165402

[12] Blaise G. and Sarjeant W. J. 1998 *IEEE Transactions on Dielectrics and Electrical Insulation* **5** 779

[13] Pan S., Min D., Wang X., Hou X., Wang L., and Li S 2019 *IEEE Transactions on Dielectrics and Electrical Insulation* **66** 549

[14] Fabiani D., Montanari G. C., Laurent C., and Teyssedre G., 2008 *IEEE Electrical Insulation Magazine* **24** 4455499

[15] Alison J. M. and Hill R. M. 1994 *Journal of Physics D: Applied Physics* **27** 1291

[16] Roy Le S., Teyssèdre G., and Laurent C. 2016 *IEEE Transactions on Dielectrics and Electrical Insulation* **23** 2361

[17] Roy Le S., Teyssedre G., Laurent C., Montanari G. C., and Palmieri F. 2004 *Journal of Physics D: Applied Physics* **37** 298

[18] Zhan Y., Chen G., and Hao M. 2019 *IEEE Transactions on Dielectrics and Electrical Insulation* **2** 43

[19] Roy Le S., Teyssedre G., Laurent C., Montanari G. C., and Palmieri F. 2006 *Journal of Physics D: Applied Physics* **39** 1427
[20] Tian J., Zou J., Wang Y., Liu J., Yuan J., and Zhou Y. 2008 *Journal of Physics D: Applied Physics* **41** 195416
[21] Xue J., Zhang Z., Zhu M., Zhao Y., and Ding L. 2021 *Journal of Physics D: Applied Physics* **54** 485501
[22] Roy Le S., Teyssedre G., Laurent C. 2016 *IEEE Transactions on Dielectrics and Electrical Insulation* **23** 2361
[23] Lan L., Wu J., Yin Y., and Zhong Q. 2014 *Japanese Journal of Applied Physics* **53** 071702
[24] Che H., and Li Z. 2013 *Jicable-HVDC, Perpignan, France* pp 04
[25] Lan L., Wu J., Yin Y., Li X., and Li Z. 2014 *IEEE Transactions on Dielectrics and Electrical Insulation* **21** 1784
[26] Hoang A., Serdyuk Y. V, and Gubanski S. 2016 *Polymers* **8** 103
[27] Min D., Cho M., Li S. T., and Khan A. R. 2012 *IEEE Transactions on Dielectrics and Electrical Insulation* **19** 2206
[28] Meunier M., Quirke N., and Aslanides A. 2001 *Journal of Chemical Physics* **115** 287
[29] Teyssedre G. and Laurent C. 2005 *IEEE Transactions on Dielectrics and Electrical Insulation* **12** 857
[30] Wu J. D., Lan L., Li Z.., and Yin Y. 2014 *in International Symposium on Electrical Insulating Materials* pp. 65
[31] Zhou G. Y., Wu J. D., and Zhang Y. 2019 *IEEE Transactions on Dielectrics and Electrical Insulation* **26** 1981
[32] He D., Wang X., Liu H., Li Q., and Teyssèdre G. 2018 *IEEE Transactions on Dielectrics and Electrical Insulation* **2** 25